GEORGIA INSTITUTE OF TECHNOLOGY
OFFICE OF CONTRACT ADMINISTRATION
SPONSORED PROJECT INITIATION

Date: August 24, 1979

Project Title: UV Laser Induced Florescence Detection of the Atmospheric Trace Gases NO, SO_2, CH_2O

Project No: G-35-658

Project Director: Dr. Douglas D. Davis

Sponsor: National Science Foundation

Agreement Period: From 7/1/79 Until 12/31/81 (Grant Period)

Type Agreement: Grant No. ATM-7906556, dated 8/3/79

Amount:
$129,000 NSF (G-35-658)
34,067 GIT (G-35-343)
$163,067 Total

Reports Required: Annual Progress Report(s); Final Project Report

Sponsor Contact Person (s):

Technical Matters

NSF Program Official
Robert J. O'Neal
Program Director
Atmospheric Chemistry
Atmospheric Research Section
Directorate for Astronomical Atmospheric, Earth, and Ocean Sciences
National Science Foundation
Washington, D. C. 20550

202/632-1976

Contractual Matters
(thru OCA)

NSF Grants Official
Terry J. Pacovsky
AAEO/ASRA Branch, Section I
Division of Grants and Contracts
Directorate for Administration
National Science Foundation
Washington, D. C. 20550

202/632-5892

Defense Priority Rating: N/A

Assigned to: Geophysical Sciences (School/Laboratory)

COPIES TO:

Project Director
Division Chief (EES)
School/Laboratory Director
Dean/Director—EES
Accounting Office
Procurement Office
Security Coordinator (OCA)
Reports Coordinator (OCA)

✓Library, Technical Reports Section
EES Information Office
EES Reports & Procedures
Project File (OCA)
Project Code (GTRI)
Other: _____

GEORGIA INSTITUTE OF TECHNOLOGY OFFICE OF CONTRACT ADMINISTRATION

SPONSORED PROJECT TERMINATION SHEET

2- SR-337 Covers SR-349

Date 9/8/82

Project Title: UV ~~Laser~~ Laser Induced ~~Florescence~~ Fluorescence Detection of the Atmospheric Trace Gases NO, SO_2, CH_2O

Project No: G-35-658

Project Director: Doug Davis

Sponsor: National Science Foundation

Effective Termination Date: 12/31/81

Clearance of Accounting Charges: _____

Grant/Contract Closeout Actions Remaining:

- [x] Final Invoice and Closing Documents
- [ ] Final Fiscal Report
- [x] Final Report of Inventions (Positive only)
- [x] Govt. Property Inventory & Related Certificate
- [ ] Classified Material Certificate
- [ ] Other _____

Assigned to: GEO SCI (School/Laboratory)

COPIES TO:

Administrative Coordinator	Research Security Services	EES Public Relations (2)
Research Property Management	Reports Coordinator (OCA)	Computer Input
Accounting	Legal Services (OCA)	Project File
Procurement/EES Supply Services	Library	Other _____

G-35-658

NATIONAL SCIENCE FOUNDATION
Washington, D.C. 20550

FINAL PROJECT REPORT
NSF FORM 98A

PLEASE READ INSTRUCTIONS ON REVERSE BEFORE COMPLETING

PART I–PROJECT IDENTIFICATION INFORMATION

1. Institution and Address	2. NSF Program	3. NSF Award Number
Georgia Institute of Technology School of Geophysical Sciences Atlanta, Georgia 30332	Atmospheric Sciences	ATM-7906556
	4. Award Period From 7/1/79 To 12/31/81	5. Cumulative Award Amount $129,000

6. Project Title
UV Laser Induced Fluorescence Detection of the Atmospheric Trace Gases NO, SO_2, and CH_2O

PART II–SUMMARY OF COMPLETED PROJECT *(FOR PUBLIC USE)*

During the time period of July 1979 to December 1981, we were completely successful in developing both NO and SO_2 LIF detection systems. Using the single photon LIF method, we have determined that under atmospheric conditions the limits of detection for NO and SO_2 should be 3 and 4 pptv, respectively. Laboratory calibration curves for both species currently go down to ∿20 pptv. Both the NO and SO_2 SP-LIF systems have also undergone initial field testing at Georgia Tech's new Stone Mt. Field Sampling Station. More extensive testing is due to begin in October of 1982. Details on the SP-LIF NO and SO_2 systems can be found in the enclosed reprint from the Journal of Applied Optics.

In addition to the SP-LIF NO technique developed, we have also in this time period been able to demonstrate what appears to be an even more selective and more sensitive LIF method for detecting NO. This new approach involves the use of two laser photons which sequentially pump the NO molecule into a high lying bonding excited state. The resulting fluorescence is therefore blue shifted relative to the lowest laser pumping line. The latter sampling configuration results in a major reduction in the background non-resonant fluorescence noise by ∿10^5 and this TP-LIF system becomes a signal limited system rather than S/N limited. The limit-of-detection for the TP-LIF technique now is estimated (based on a laboratory calibration curve) at ∿.3 pptv. For details on this new system see the enclosed reprint from Optics Letters.

Concerning the SP-LIF system for detecting CH_2O, only minimal laboratory progress has been made on this project due to the time invested in the TP-LIF NO system. The latter effort was not part of our original proposal and came as a spin-off from our early work on the SP-LIF NO system. However, all hardware for the CH_2O has now been acquired, and this system should be fully laboratory tested within the next 12 months. The continuation of this effort will be carried out using resources from other sponsors as well as those contributed by Georgia Tech.

PART III–TECHNICAL INFORMATION *(FOR PROGRAM MANAGEMENT USES)*

1. ITEM *(Check appropriate blocks)*	NONE	ATTACHED	PREVIOUSLY FURNISHED	TO BE FURNISHED SEPARATELY TO PROGRAM	
				Check (√)	Approx. Date
a. Abstracts of Theses	√				
b. Publication Citations		√			
c. Data on Scientific Collaborators	√				
d. Information on Inventions	√				
e. Technical Description of Project and Results		√			
f. Other *(specify)*					

2. Principal Investigator/Project Director Name *(Typed)*	3. Principal Investigator/Project Director Signature	4. Date
		8/28/82

NSF Form 98A (5-78) Supersedes All Previous Editions

Form Approved OMB No. 99R0013

INSTRUCTIONS FOR FINAL PROJECT REPORT
(NSF FORM 98A)

This report is due within 90 days after the expiration of the award. It should be submitted in two copies to:

National Science Foundation
Division of Grants and Contracts
Post-Award Projects Branch
1800 G Street, N.W.
Washington, D.C. 20550

INSTRUCTIONS FOR PART I

These identifying data items should be the same as on the award documents.

INSTRUCTIONS FOR PART II

The summary (about 200 words) must be self-contained and intelligible to a scientifically literate reader. Without restating the project title, it should begin with a topic sentence stating the project's major thesis. The summary should include, if pertinent to the project being described, the following items:

- The primary objectives and scope of the project.
- The techniques or approaches used only to the degree necessary for comprehension.
- The findings and implications stated as concisely and informatively as possible.

This summary will be published in an annual NSF report. Authors should also be aware that the summary may be used to answer inquiries by nonscientists as to the nature and significance of the research. Scientific jargon and abbreviations should be avoided.

INSTRUCTIONS FOR PART III

Items in Part III may, but need not, be submitted with this Final Project Report. Place a check mark in the appropriate block next to each item to indicate the status of your submission.

a. Self-explanatory.
b. For publications (published and planned) include title, journal or other reference, date, and authors. Provide two copies of any reprints as they become available.
c. Scientific Collaborators: provide a list of co-investigators, research assistants and others associated with the project. Include title or status, e.g. associate professor, graduate student, etc.
d. Briefly describe any inventions which resulted from the project and the status of pending patent applications, if any.
e. Provide a technical summary of the activities and results. The information supplied in proposals for further support, updated as necessary, may be used to fulfill this requirement.
f. Include any additional material, either specifically required in the award instrument (e.g. special technical reports or products such as films, books, studies) or which you consider would be useful to the Foundation.

Sequential two-photon-laser-induced fluorescence: a new method for detecting atmospheric trace levels of NO

J. Bradshaw and D. D. Davis

School of Geophysical Sciences, Georgia Institute of Technology, Atlanta, Georgia 30332

Received January 13, 1982

Sequential two-photon-laser-induced fluorescence (TP-LIF) in NO has been achieved by using 226-nm radiation to excite the $X^2\Pi \rightarrow A^2\Sigma$ transition followed by excitation of the $A^2\Sigma \rightarrow D^2\Sigma$ transition using the fundamental output of a Nd:YAG laser at 1064 nm. The resulting fluorescence was monitored at wavelengths as low as 187 nm ($D^2\Sigma \rightarrow X^2\Pi$ transition), thus permitting major discrimination against conventional noise sources as encountered in single-photon-laser-induced fluorescence (SP-LIF) systems. Also, since the 226-nm radiation used in the TP-LIF method is generated in the same manner as in the SP-LIF technique (i.e., the sum-frequency mixing of 288- with 1064-nm radiation), the two-photon sequential-pumping scheme requires no major extra optical hardware. Although the final optimization of the TP-LIF NO method has not yet been completed, extrapolations based on currently measured signal and noise levels suggest a detection sensitivity level of 3 parts in 10^{13} (0.3 pptv) under atmospheric conditions. This would represent approximately a 25-fold increase in sensitivity over the SP-LIF NO technique.

Earlier laser efforts at detecting NO under atmospheric conditions of composition and pressure have involved single-photon excitation of NO with the monitoring of fluorescence at wavelengths that are red shifted relative to the excitation wavelength.[1] The sequential two-photon-laser-induced fluorescence (TP-LIF) technique being reported on here has potentially far greater sensitivity than the single-photon method because the resulting fluorescence is blue shifted relative to the shortest laser wavelength used to pump NO optically.

The relevant energy levels employed in the two-photon excitation of NO are shown in Fig. 1. (Data on the natural radiative lifetime of NO and the appropriate quenching rates for different electronic states are given in Table 1.) For this system, it can be seen that a significant fraction of the fluorescence, monitored at λ_3, occurs at a lower wavelength than both the λ_1 and λ_2 laser excitation wavelengths. As is shown in Fig. 2, this scheme thus permits discrimination against all Rayleigh- and Stokes-shifted Raman noise sources and white fluorescence from aerosols and chamber walls as well as fluorescence from other trace gases, such as that from SO_2. The dominant noise sources in the TP-LIF method now appear to be anti-Stokes Raman scatter, resulting from N_2 and O_2, and weak multiphoton-absorption processes by unidentified gas-phase impurities. Evaluation of the magnitude of this real photon noise (relative to the signal) is easily achieved by simply tuning the dye laser (in actual fact the 226-frequency-mixed wavelength) ~0.02 nm off the NO absorption line.[2] Although noise tests have not yet been completed on the NO system by using fast-collection optics, based on other two-photon systems in our laboratory also involving blue-shifted fluorescence,[4] the real photon noise from the TP-LIF NO system is predicted to be 10^5 to 10^6 times lower than that observed in the single-photon-laser-induced fluorescence (SP-LIF) NO system—both being normalized to the same input energy at 226 nm and for the same transmission in collection optics. Thus, unlike SP-LIF systems, all of which tend to be signal-to-noise limited under realistic atmospheric sampling conditions, the TP-LIF system is expected to be a signal-limited system under typical sampling conditions.

The TP-LIF signal strength D_{λ_3} (e.g., detected signal photons per laser shot) can be expressed in terms of several convenient efficiency terms, namely,

$$D = E_{\lambda_1} \times E_{\lambda_2} \times E_f \times E_d \times E_e \times V \times [\mathrm{NO}]. \quad (1)$$

Each of these terms can be assigned physical significance as follows:

$$E_{\lambda_1} = \begin{pmatrix}\text{optical pumping}\\ \text{efficiency}\\ \text{at } \lambda_1\end{pmatrix} = \left[1 - \exp - \left(\frac{P_{\lambda_1}\sigma_{\lambda_1}}{a_{\lambda_1}}\right)\right] \times f_i \times S_{\lambda_1}, \quad (2)$$

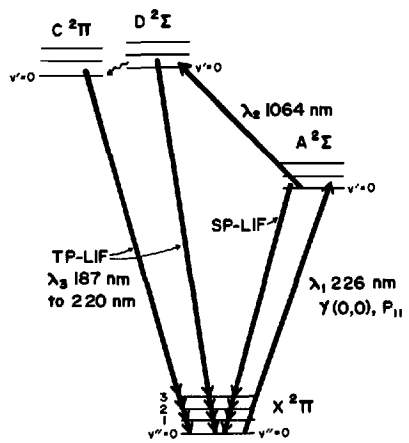

Fig. 1. NO energy-level diagram showing those transitions involved in the sequential two-photon-laser-induced fluorescence detection scheme.

Table 1. Spontaneous Emission and Quenching Frequency Factors in One Atmosphere of Air[a]

Upper State	$A^2\Sigma$	$C^2\Sigma$ (sec^{-1})	$D^2\Sigma$ (sec^{-1})
k_f to $X^2\Pi$	5×10^6 sec^{-1}[b]	5×10^7[b]	4×10^7[b]
k_f to $A^2\Sigma$	–	3.5×10^7[b]	9.5×10^6[b]
k_d ($v' < 1$)	No predissociation for $v' < 4$[b]	1.7×10^9[b]	$<8 \times 10^6$[b]
$k_q[M]$	1×10^9 sec^{-1}[c]	4×10^{10}[b]	$\sim 2 \times 10^9$[d]

[a] The composition has been taken to be 590-Torr N_2, 150-Torr O_2, and 10-Torr H_2O.
[b] Taken from Ref. 5.
[c] Taken from an average of data in Refs. 6 and 7.
[d] Taken from Ref. 8.

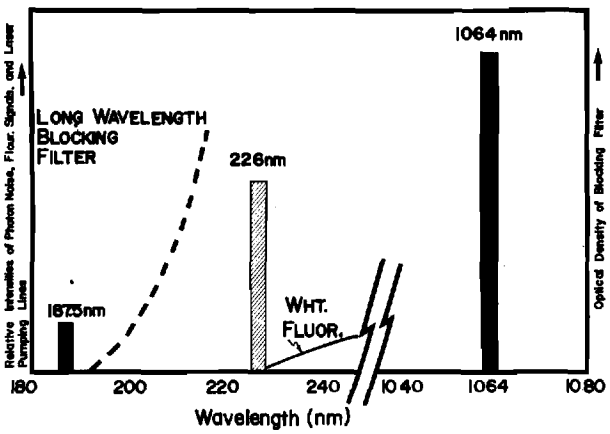

Fig. 2. Qualitative presentation of the two-photon-laser-induced detection scheme showing the spectral location of the laser pumping lines, the monitored fluorescence, white-noise fluorescence, and the cutoff characteristics of a future long-wavelength cutoff filter. It is not intended that absolute photon fluxes be estimated from this graph.

$$E_{\lambda_2} = \begin{pmatrix}\text{optical pumping}\\ \text{efficiency}\\ \text{at } \lambda_2\end{pmatrix} = \left[1 - \exp - \left(\frac{P_{\lambda_2}\sigma_{\lambda_2}}{a_{\lambda_1}}\right)\right] \times \frac{a_{\lambda_1}}{a_{\lambda_2}} \times R \times S_{\lambda_2}, \quad (3)$$

$$E_f = \begin{pmatrix}\text{fluorescence}\\ \text{efficiency}\end{pmatrix} = \frac{k_f}{k_f + k_d + k_q[M]}, \quad (4)$$

$$E_d = \begin{pmatrix}\text{optical}\\ \text{detection}\\ \text{efficiency}\end{pmatrix} = \gamma_{\lambda_3} \times Y_{\lambda_3} \times Z_{\lambda_3} \times \phi_{\lambda_3}, \quad (5)$$

$$E_e = \begin{pmatrix}\text{electronic}\\ \text{detection}\\ \text{efficiency}\end{pmatrix} = \frac{\text{PMT signal pulses counted}}{\text{PMT signal pulses emitted}}, \quad (6)$$

$$V = \begin{pmatrix}\text{volume of}\\ \text{sampling}\\ \text{region}\end{pmatrix} = a_{\lambda_1} \times l \text{ for } a_{\lambda_1} < a_{\lambda_2}. \quad (7)$$

Here P_{λ_1} and P_{λ_2} represent the number of laser photons per laser shot at λ_1 and λ_2, respectively; σ_{λ_1} and σ_{λ_2} are the effective absorption cross sections for NO at λ_1 and λ_2; f_i is the fraction of the total NO population in quantum states that can be pumped at 226 nm with a laser linewidth $\Delta\lambda$; k_f is the reciprocal of the natural lifetime; k_d is the first-order rate constant for dissociation; k_q is the biomolecular electronic-quenching-rate constant; $[M]$ is the concentration of the quenching species; γ_{λ_3} is the fraction of total fluorescence falling within the optical-transmission window; Y_{λ_3} is the optical-collection efficiency; Z_{λ_3} is the optical-filter transmission factor; ϕ_{λ_3} is the quantum efficiency of the photomultiplier tube (PMT) at λ_3; and a_{λ_1} and a_{λ_2} are the cross-sectional areas of the λ_1 and λ_2 laser beams. S_{λ_1} and S_{λ_2} are saturation parameters, which can be taken to be unity under low laser-energy-density conditions and/or with small cross sections for the absorbing species. Bradshaw *et al.*[1] have demonstrated this to be the case for S_{λ_1} for 226-nm laser energies up to 1 mJ involving a 5-mm-diameter beam. S_{λ_2} has not been quantitatively assessed, but it appears that the cross section for the $A^2\Sigma \rightarrow D^2\Sigma$ transition, when 1064-nm radiation is used, is quite small; thus the value of S_{λ_2} is likely to be close to unity. This assumption, however, will need to be verified. The quantity R in the expression for E_{λ_2} defines the fraction of NO molecules that have been pumped into the $A^2\Sigma$ state that survives quenching by N_2 and O_2 and therefore is excited into the $D^2\Sigma$ state. This quantity cannot be evaluated directly at this time because of the absence of a known cross section for 1064-nm absorption from the $A^2\Sigma$ state. Thus the term E_{λ_2} has here been evaluated by experimentally determining the quantities D_{λ_3}, V, [NO], E_d, and E_e and using calculated values for E_{λ_1} and E_f.

The TP-IF system used in this study is shown in Fig. 3. In this system, the Nd:YAG laser type was an ILS NT-572, whereas the pulsed dye laser was designed and built by Quanta Ray. The latter dye-laser unit was operated in an oscillator–end-pumped-amplifier configuration and was flied with R610 dye.

An evaluation of each of the efficiency terms in Eq. (1), for the experimental system shown in Fig. 1, gave $E_{\lambda_1} = 0.013$, $E_{\lambda_2} = 0.0052$, $E_f = 0.020$, $E_d = 3 \times 10^{-7}$, $E_e = 0.9$, $V = 0.04$ cm^3. The signal strength D_{λ_3} for an NO concentration of 2.5×10^{12} molecules cm^{-3} (100 ppbv) is calculated to be

$$D_{\lambda_3} = 220 \text{ photons/6000 laser shots.}$$

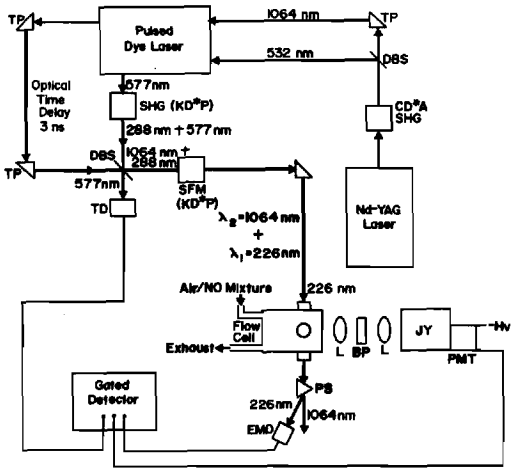

Fig. 3. Sequential two-photon-laser-induced fluorescence experimental setup: BP, bandpass filter; DBS, dichroic beam splitter; EMD, energy-monitor diode; L, lens; PMT, photomultiplier tube; PS, 60° prism separator; SFM, sum-frequency-mixing crystal; SHG, second-harmonic-generating crystal; TD, trigger diode; TP, turning prism; JY, Jobin-Yvon double monochromator.

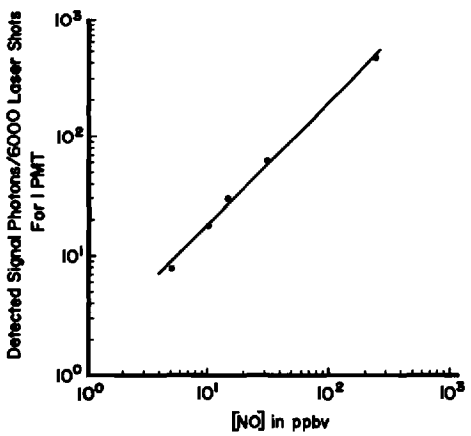

Fig. 4. Two photon-laser-induced fluorescence calibration curve for NO: $\lambda_1 = 650\ \mu$J (226 nm), $\lambda_2 = 75$ mJ (1064 nm). Signals are reported for a 1-atm-pressure air mixture.

An experimental calibration curve showing the linearity of the TP-LIF NO system over 2 orders of magnitude in NO concentration is shown in Fig. 4. These data were recorded under atmospheric conditions of pressure and composition. The signal-limited nature inherent in the TP-LIF technique permits linear gains in detection sensitivity with increases in the efficiency of the collection optics, laser energy, etc., compared with the square-root gain in detection sensitivity inherent in signal-to-noise-limited methods. By a judicious choice of hardware, namely, a fast far-UV solar-blind PMT, high-transmission chemical-solution filters, high-speed-collection optics, and a somewhat higher laser energy at 226 nm (i.e., 1.2 versus 0.65 mJ), we expect to achieve the following values for each of the above efficiency terms: $E_{\lambda_1} = 0.024$, $E_{\lambda_2} = 0.0052$, $E = 0.020$, $E_d = 1.3 \times 10^{-5}$, $E_e = 0.9$, $V = 0.25$ cm^3, where the change in the value of V reflects the improvement in the fraction of the laser beam (length and width) from which fluorescence is to be sampled rather than a change in the laser-beam diameter. The increase in the value of E_d, on the other hand, reflects the calculated improvement in the efficiency with which fluorescence from *a given volume/element* in the laser beam will be sampled using f:1 collection optics in conjunction with chemical filters rather than the J-Y double-monochromator system. In the above improved experimental system (currently under development in our laboratory), we would calculate a signal strength for an NO concentration of 100 ppbv of

$$D_{\lambda_3} = 1.1 \times 10^5 \text{ photons/6000 laser shots.}$$

This represents an improvement of ~500-fold over the system used here initially to assess the TP-LIF technique. In addition, if six PMT's are utilized rather than one (for purposes of airborne field sampling), the improvement in sensitivity would be ~3000-fold, again assuming that we are operating in a signal-limited NO-concentration range. Thus we now estimate that the detection limit for NO by the sequential TP-LIF method (utilizing technology currently available or under development in our laboratory) will be ~0.3 pptv for an integration time of 20 min.

In conclusion, it now appears that the sequential TP-LIF technique has the potential for detecting atmospheric NO levels as much as a factor of 25 times lower than that possible by using the SP-LIF detection method. In addition, this new technique's inherent ability to overcome conventional noise sources, e.g., Rayleigh and Stokes–Raman scatter and white-background fluorescence, suggests that it may be applicable to environments heretofore inaccessible to the SP-LIF technique as well as to other nonlaser techniques. This might involve using the TP-LIF system to measure NO in high aerosol environments, such as in clouds.

References

1. J. D. Bradshaw, M. O. Rodgers, and D. D. Davis "Single photon/laser-induced fluorescence detection of NO and SO_2 under conditions of atmospheric composition and pressure" Appl. Opt. (to be published).
2. In actual fact, several NO lines are excited at the P_{11} bandhead, the average J value being 15/2.
3. M. O. Rodgers, K. Asai, and D. D. Davis, "Photofragmentation-laser-induced fluorescence: a new method for detecting atmospheric trace gases," Appl. Opt. **19**, 3597 (1980).
4. D. D. Davis, M. O. Rodgers, K. Liu, and J. D. Bradshaw, "Photofragmentation/laser-induced fluorescence detection of NO_2 under conditions of atmospheric composition and pressure" Appl. Opt. (to be published).
5. S. Cieslik and M. Nicolet, "The aeronomic dissociation of nitric oxide," Planet. Space Sci. **21**, 925 (1973).
6. L. A. Melton and W. Klemperer, "Quenching of NO $A^2\Sigma^+$ by O_2 $X^2\Sigma_g^{-11}$," Planet. Space Sci. **20**, 157 (1972).
7. I. S. McDermid and J. B. Laudenslager, "Radiative lifetimes and electronic quenching rate constants for single-photon-excited rotational levels of NO ($A^2\Sigma^+$, $v' = 0$)," J. Quant. Spectrosc. Radiat. Transfer (to be published).
8. Y. Haas and M. Asscher, "Photoselective chemistry," *Advances in Chemical Physics*, Vol. XLVII, J. Jortner, R. D. Levine, and S. A. Rice, eds. (Wiley, New York, 1981).

Single photon laser-induced fluorescence detection of NO and SO_2 for atmospheric conditions of composition and pressure

J. D. Bradshaw, M. O. Rodgers, and D. D. Davis

Reported here are laboratory results from a laser-induced fluorescence (LIF) study of the molecules NO and SO_2 in which both the selectivity and sensitivity of the LIF method are examined. The laser excitation of these molecules occurred at 226 and 222 nm, respectively. The laser system employed consisted of a Nd:YAG-driven Quanta-Ray PDL dye laser, the fundamental of which was frequency doubled, and this output, in turn, was then frequency mixed with the Nd:YAG fundamental at 1064 nm. Two different dyes were required for generating the 226- and 222-nm wavelengths. To make these results as relevant as possible to the ultimate development of an atmospheric airborne field sampling system all experiments were carried out in atmospheric conditions of pressure and composition. In addition to the experimental data provided there has also been presented a theoretical assessment of the signal strength for both the NO and SO_2 LIF systems, and these results have been compared with the experimentally measured values. Current state-of-the-art technology would suggest that both NO and SO_2 can be measured by the LIF technique in atmospheric conditions at concentration levels of a few pptv.

I. Introduction

Of principal interest in this paper will be the presentation of new laboratory results involving the potential extension of the laser-induced fluorescence method to the detection of atmospheric NO and SO_2. Both molecules have recently been receiving increasing scrutiny from government agencies due to their role in the growing environmental problem now labeled acid rain. This phenomenon, first identified as a serious environmental threat by European scientists during the middle 1950s (Barnett and Brodin[1]) and by U.S. scientists in the early 1970s (Likens[2]), is now believed to be the end product of the atmospheric chemical conversion of NO to HNO_3 and SO_2 to H_2SO_4. In addition, however, to the precursor role that NO plays in the acid rain question, this molecule is also a pivotal species in several fast photochemical atmospheric cycles involving such species as O_3 and OH. The hydroxyl radical, in particular, is now thought to control the atmospheric lifetime of numerous trace gases, i.e., CO, NO_2, SO_2, H_2S, $(CH_3)_2S$, CF_2HCl, CCl_3CH_3, CH_4, and other higher molecular-weight hydrocarbons.

The authors are with Georgia Institute of Technology, School of Geophysical Sciences, Atlanta, Georgia 30332.

Received 29 January 1982.
0003-6935/82/142493-08$01.00/0.

Recognizing the atmospheric importance of the gases NO and SO_2, not surprisingly several real-time sampling techniques have been developed for detecting these trace gases. Most of these techniques, however, have been configured for measurements involving concentration levels in the ppbv–ppmv range. For measuring subppbv NO concentration levels, Ridley and Howlett,[3] Schiff *et al.*,[4] and McFarland *et al.*,[5] have developed higher sensitivity chemiluminescence detectors which again, however, are based on the chemiluminescence produced when NO reacts with added excess O_3. Concerning subppbv levels of SO_2, the most successful effort to date for real-time measurements has been that by Maroulis *et al.*[6,7] These investigators have used gas chromatographic separation to isolate various possible sulfur compounds present in an incoming gas stream and then inject the output from the GC column into a flame photometric detector where the emission from S_2 is monitored. To maximize the detection sensitivity of this method preconcentration of the sulfur compound of interest is carried out by flowing the sampled airstream through a U trap immersed in liquid argon. After a few minutes collection time the contents are rapidly warmed and injected onto the GC column for separation.

Presented in this paper are laboratory results concerned with the detection of NO and SO_2 using the single-photon laser-induced fluorescence technique. Previous efforts involving the use of LIF to monitor these two molecules have typically involved low pres-

sures of diluent gases and/or very high concentrations of the primary species NO and SO_2 (Zacharias *et al.*,[8] Eckbreth *et al.*,[9] and Bode *et al.*[10]). This study is intended to demonstrate the feasibility of using this methodology in the detection of NO and SO_2 at concentration levels and conditions present in the lower atmosphere. Since this technique is based on a direct spectroscopic detection method, it necessarily suggests very high selectivity. As will be seen later in the text, the method also turns out to be highly sensitive for detecting both NO and SO_2.

II. Theoretical Treatment of Single-Photon LIF Signal Strength

Taking the generalized case of a single-photon (SP) LIF system to be represented by

$$AB + h\nu_1 \rightarrow AB^*,$$
$$AB^* \rightarrow AB + h\nu_2,$$
$$AB^* + M \rightarrow AB + M^{\ddagger},$$

the basic mathematical relationship that defines the signal strength for such a system is given by

D_{λ_2}(detected λ_2 photons) =
(total no. of λ_2 photons emitted, P_{λ_2})
× (optical detection efficiency for λ_2 photons, E_d)
× (electronic detection efficiency, E_e),

or in abbreviated form

$$D_{\lambda_2} = P_{\lambda_2} \times E_d \times E_e. \tag{1}$$

The simplest term in Eq. (1), E_e, represents the fraction of the total photomultiplier tube (PMT) signal detected by the processing electronics. In typical operating conditions, where the noise in an LIF system is greater than one photon/laser shot (see, for example, the discussion by Davis *et al.*[11]), the value of E_e is close to unity. However, in the event that photon-counting methods are used, the voltage threshold on the counter/discriminator network may be set to optimize the number of signal photons counted relative to low-level electrical noise. Thus the latter operation will usually result in a small but measurable rejection of signal photons, and E_e will take on a value somewhat less than unity.

The second term in Eq. (1), the optical detection efficiency, may be expanded as follows:

E_d = (fraction of total fluorescence within the optical sampling window, γ_{λ_2})
× (collection optics efficiency factor at λ_2, Y_{λ_2})
× (filter transmission factor at λ_2, Z_{λ_2})
× (quantum efficiency of the PMT, ϕ_{λ_2}),

or

$$E_d = \gamma_{\lambda_2} \times Y_{\lambda_2} \times Z_{\lambda_2} \times \phi_{\lambda_2}. \tag{2}$$

The first term in Eq. (1), P_{λ_2}, is more complex and can be further defined as

P_{λ_2} = (total number of λ_1 photons absorbed, N_{λ_1})
× (fluorescence efficiency of AB^*, E_f),

or

$$P_{\lambda_2} = N_{\lambda_1} \times E_f. \tag{3}$$

The number of λ_1 photons absorbed, N_{λ_1}, may be expressed as

N_{λ_1} = (total number of AB molecules within the sampling volume, C)
× (fraction of molecules in quantum state i, absorbing photons, E_{λ_1}). (4)

The first term in Eq. (4) can be expressed in terms of the concentration of AB and the sampled volume element V, i.e.,

$$C = (AB) \times V, \tag{5}$$

where V is defined by the product of the laser beam cross-sectional area a_{λ_1} and the effective laser path length l over which fluorescence is sampled. The second term, the fluorescence pumping efficiency E_{λ_1} is given by

$$E_{\lambda_1} = \left[1 - \exp - \left(\frac{P_{\lambda_1} \times \sigma_{\lambda_1}}{a_{\lambda_1}}\right)\right] \times f_i \times S_{\lambda_1}. \tag{6}$$

Here P_{λ_1} is the number of λ_1 laser photons per laser shot, σ_{λ_1} is the effective absorption cross section for the molecule AB in the i quantum state, and a_{λ_1} is the cross-sectional area of the λ_1 laser beam. Taking f_i as the fraction of the total AB population that is in the ith quantum state, it is frequently possible to pump more than a single quantum state via a narrow line laser, thus increasing the magnitude of the f_i term accordingly. The value of σ_{λ_1} may or may not be altered by there being multiple quantum states that can be pumped. S_{λ_1} is an optical saturation parameter which typically can be taken to be unity unless very high spectral irradiances (high pumping power) are employed and/or the absorption process has a very large cross section (see detailed discussion later in the text for the specific molecules NO and SO_2).

Returning to the second term in Eq. (3), E_f, this quantity can be expanded according to Eq. (7), i.e.,

$$E_f = \begin{pmatrix}\text{fraction of excited } AB \text{ molecules} \\ \text{producing fluorescence}\end{pmatrix} = \frac{k_f}{[k_f + k_d + \Sigma k_q(M)]}, \tag{7}$$

where k_f is the reciprocal of the natural radiative lifetime τ of AB^*, k_d is the first-order rate constant for dissociation, k_q is the bimolecular electronic quenching rate constant, and (M) is the concentration of each quenching species.

Thus based on the detailed expressions given in Eqs. (5)–(7), Eq. (3) may be rewritten in the form

$$P_{\lambda_2} = (AB) \times E_{\lambda_1} \times E_f \times V. \tag{8}$$

Substitution of Eq. (8) into Eq. (1) then gives the final form of the signal-strength expression (e.g., detected

signal photons per laser shot) for the single-photon LIF method, i.e.,

$$D_{\lambda_2} = (AB) \times E_{\lambda_1} \times E_f \times E_d \times E_e \times V. \quad (9)$$

Equation (9) represents a very useful form of the signal equation since each term can readily be assigned some physical significance. For example,

E_{λ_1} = (optical pumping efficiency at λ_1)

$$= \left[1 - \exp - \left(\frac{P_{\lambda_1} \times \sigma_{\lambda_1}}{a_{\lambda_1}}\right)\right] \times f_i \times S_{\lambda_1},$$

E_f = (fluorescence efficiency) $= \dfrac{k_f}{[k_f + k_d + \Sigma k_q(M)]}$,

E_d = (optical detection efficiency)

$= \gamma_{\lambda_2} \times Y_{\lambda_2} \times Z_{\lambda_2} \times \phi_{\lambda_2}$,

E_e = (electronic detection efficiency)

$= \dfrac{\text{PMT signal pulses counted}}{\text{PMT signal pulses emitted}}$,

V = (effective volume of sampling region) $= a_{\lambda_1} \times l$.

III. Analysis of the SP-LIF NO System

The basic approach in the LIF technique is illustrated in Figs. 1 and 2 for the case of the NO molecule. In this system it can be seen that NO is initially excited into the $v' = 0$ manifold of the $A^2\Sigma^+$ electronic state [$\gamma(0,0)$ transition] by absorption of a laser photon centered at ~226 nm. Although a very large fraction of these excited NO molecules are electronically quenched via collisions with O_2, intense fluorescence can still be observed at both the pumping wavelength as well as at several other wavelengths corresponding to transitions to the $v'' = 0$, 1, 2, and 3 levels of the $X^2\Pi$ ground state. However, since the Franck-Condon factors for all four transitions are within a factor of 2.5 of each other, the selection of the transition to be monitored must take into consideration the possible noise sources in the system. If the $\gamma(0,0)$ transition were to be monitored in fluorescence, a serious noise problem could result from Rayleigh scattering of the 226-nm pump beam.

Concerning long-wavelength shifted fluorescence (involving transitions to the $v'' = 1$, 2, 3, and 4 levels), Fig. 2 shows that, with the aid of narrow bandpass and low-wavelength cutoff filters, the Rayleigh scatter from the 226-nm pump beam can be reduced to insignificant levels. Thus, if this were the only noise source in the system, it would suggest that for transitions having nearly equal Franck-Condon factors the longest wavelength possible from the $A^2\Sigma^+$ state of NO would be the best one to monitor. In fact, a quite different noise source is frequently found to be the dominant one in this system, i.e., white fluorescence. The latter type of fluorescence can typically be represented as a continuum fluorescence spectrally shifted toward the long-wavelength side of the laser-pumping wavelength. This fluorescence may arise from a variety of sources, including the interaction of the laser-pumping radiation with the input and output windows as well as the walls of the sampling chamber. In real-world sampling conditions a significant white-fluorescence noise can also result from the interaction of the pumping radiation with atmospheric aerosols. However, as can be seen from Fig. 2, the maximum in the white-fluorescence noise is always spectrally shifted toward the red with respect to the pump wavelength; thus the optimum NO optical transition to sample, from the point of view of minimizing the noise, is one which is spectrally shifted away from the pump wavelength but to the short-wavelength side of the maximum in the white-fluorescence noise. In the case of NO this has been determined to be the (0,3) band centered at ~259 nm. In spite of this optimum spectral location, however, white fluorescence continues to be transmitted over the spectral window of the bandpass filter (e.g., ~4 nm) to the same extent as the NO fluorescence signal. This long-wavelength white-fluorescence noise is more often than not the limiting noise in single-photon LIF atmospheric-detection systems. In a few cases, however, two additional noise sources must also be dealt with. They are Stokes-Raman scatter and solar photon noise. The latter source turns out only to be a problem when sampling at wavelengths beyond 310 nm. Stokes-Raman scatter, on the other hand, is discrete in nature and,

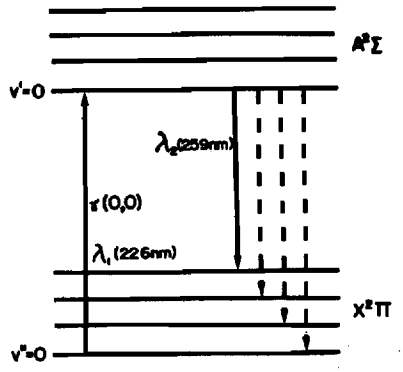

Fig. 1. Schematic energy diagram showing electronic transitions employed in the single-photon laser-induced fluorescence detection of NO.

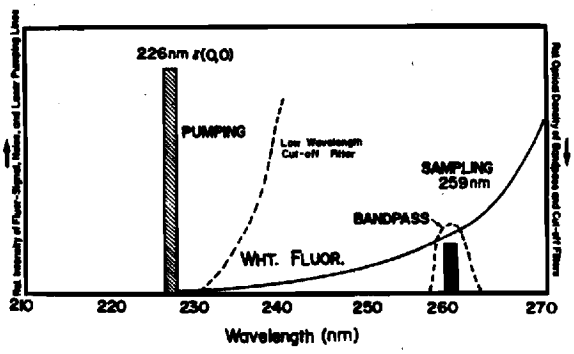

Fig. 2. Schematic diagram showing the spectral location of the excitation laser, sampled NO fluorescence, and the white-fluorescence noise. Also shown are the optical attenuating characteristics of the narrow bandpass and low-wavelength cutoff filters. (This figure is not intended to give quantitative estimates of intensities.)

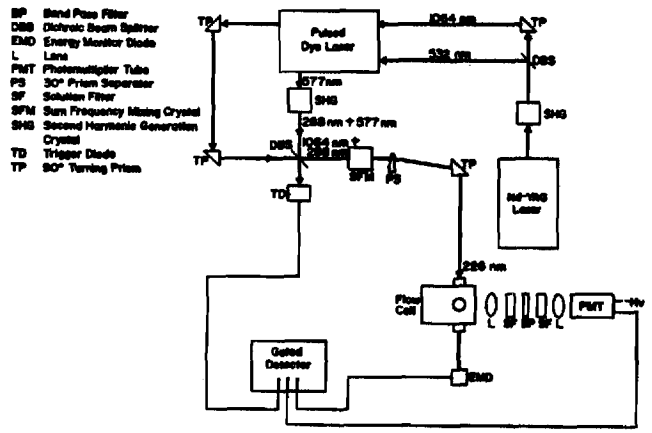

Fig. 3. Schematic diagram showing the basic laser hardware employed in the single-photon laser-induced fluorescence detection of NO and SO_2.

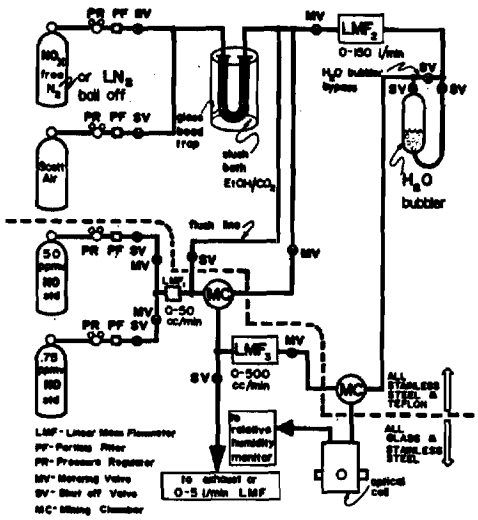

Fig. 4. Schematic diagram showing the double-dilution flow-calibration network used to establish the sensitivity limits for detecting NO and SO_2 via LIF. The critical parts of this system were fabricated from glass and passivated stainless steel.

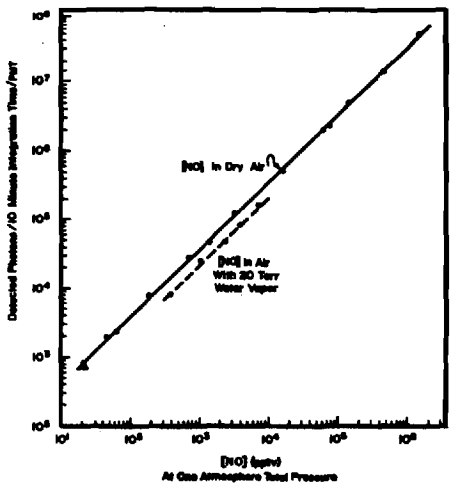

Fig. 5. Calibration curve for the detection of NO via LIF, signal (photons/10 min integration time/PMT) vs NO concentration (pptv). Dotted calibration curve is for air with 20 Torr of added water vapor. Concentration range covered 18 pptv–1 ppmv: Energy, 1 mJ at 226 nm.

therefore, can usually be reduced to insignificant levels by judiciously selecting the central wavelength and blocking characteristics on the detection system's bandpass filter. In the NO system white fluorescence has been determined to be the dominant noise source.

For purposes of illustrating several of the more important experimental characteristics of the SP-LIF method the authors have chosen to examine the NO detection system in some detail, noting that the SO_2 system is, in terms of hardware, virtually identical with the NO scheme. The basic optical hardware used in the NO LIF system is shown in schematic form in Fig. 3. The key elements here are: (1) a frequency-doubled Nd:YAG laser (ILS-NT572); (2) a 532-nm driven dye laser (Quanta-Ray PDL-1); (3) a frequency-doubling crystal; (4) a frequency-mixing crystal; and (5) a prism separator. In the specific case of NO, Fig. 3 shows that a frequency-doubling crystal is used to upconvert 577-nm radiation to 388 nm, followed by a frequency-mixing operation (using the Nd:YAG fundamental at 1064 nm) which upconverts 288-nm radiation to the desired wavelength at 226 nm. The latter approach is one also used by the Quanta-Ray Co. in their PDL Nd:YAG system.

The charge-integrating electronics employed to process the NO fluorescence signal from an EMR 541Q PMT have been previously discussed by Davis *et al.*[11] and will not be further expanded on here. The collection optics in the NO system consisted of two $f/1.4$ quartz lenses between which were sandwiched a 4-nm bandpass filter (centered at 259 nm) and low- and long-wavelength solution cutoff filters made up of ethyl bromides and 2,7-dimethyl; 3,6-diazocyclohepta; and 2,6-dieneperchlorate, respectively.

To establish known concentrations of NO, a dual-dynamic flow system was set up in which primary and secondary NO standards of 50 and 0.75 ppmv were connected into the flow system through Tel-Dyne Hastings precision-linear mass-flowmeters. This all-glass and passivated stainless steel system is shown in schematic form in Fig. 4. It will be noticed that in this system provision has also been made to add known quantities of H_2O to the gas stream to simulate a highly variable tropospheric environment. In the case of NO a variation in the water level from 0 to 20 Torr resulted in a calibration curve [i.e., (NO) vs fluorescence signal] which differed from dry air by a factor of 1.6 (see Fig. 5). This small but reproducible effect has been shown to be due to the strong electronic quenching of NO* by H_2O and indicates that the electronic quenching-rate constant for the $A^2\Sigma$ NO state by H_2O is faster than gas kinetics. Our measurements give a value of $7.4 \pm 1.4 \times 10^{-10}$ cm^3 molecule^{-1} sec^{-1} based on a $k_q(O_2)$ value of 1.5×10^{-10} cm^3 molecule^{-1} sec^{-1} (average of McDermid and Laudenslager,[12] and Melton and Klemperer[13]).

The k_q (H_2O) estimated here is thus seen to be in a very good agreement with that recently measured by McDermid and Laudenslager[12] of $7.6 \pm 0.7 \times 10^{-10}$ cm^3 molecule^{-1} sec^{-1}.

It can also be seen from Fig. 5 that the measured fluorescence signal is linear with NO concentration over ~5 orders of magnitude. In fact there is no fundamental limitation which would preclude this linearity from extending over 6 or more orders of magnitude provided that known optical attenuators were to be inserted in the collection optics or, alternatively, the gain on the PMT were to be systematically reduced, both being quite feasible.

The evaluation of the efficiency terms in Eq. (9) and the subsequent comparison of the calculated value of D_{λ_2} with that given experimentally in Fig. 5 can currently be carried out at the semiquantitative level. In the case of the SP-LIF NO system this is due primarily to the uncertainty in evaluating the collection optics efficiency factor Y_{λ_2} (in combination with defining the effective sampling volume V) and to some uncertainty yet remaining in evaluating the effective-absorption cross section for NO based on our specific laser system. In spite of these shortcomings the values of E_{λ_1}, E_f, and E_e can be calculated as given below:

E_{λ_1} = (optical pumping efficiency at 226 nm) = 1.4×10^{-2},

E_f = (fluorescence efficiency) = 6.1×10^{-3},

E_e = (electronic detection efficiency) = 1.0.

In the above calculation of E_{λ_1} a value of 7% was estimated for f_i in sampling conditions where the laser was spectrally tuned to the P_{11} NO bandhead. The value of S_{λ_1}, on the other hand, was experimentally assessed to be 1.0 ± 0.15 by systematically measuring the fluorescence signal as a function of the input laser energy, the latter being varied over the range of 0.2–1.0 mJ. The pressure-broadened effective-absorption cross section was experimentally measured as $\sigma_{\lambda_1} \times f_i$. Its value was determined to be 1.3×10^{-18} cm^2 based on a laser linewidth profile which partially and/or fully overlapped the rotational states $J = 7\frac{1}{2}, 8\frac{1}{2}, 9\frac{1}{2}$, and $10\frac{1}{2}$. Thus using our estimated value of 7% for f_i gives 1.9×10^{-17} cm^2 for the value of σ_{λ_1}. In the evaluation of E_f the natural radiative lifetime was taken to be 210 nsec (average of McDermid and Laudenslager[12] and Brzozowski *et al.*[14]); $k_q(O_2) = 1.5 \times 10^{-10}$ cm^3 molecule^{-1} sec^{-1} (average of McDermid and Laudenslager[12] and Melton and Klemperer[13]); and $k_q(N_2) = 8.3 \times 10^{-14}$ cm^3 molecule^{-1} sec^{-1} (average of McDermid and Laudenslager[12] and Callear and Pilling[15]). Determining the magnitude of E_d required an estimation of Y_{λ_2}, which for our system was experimentally estimated to be 0.008. Based on available Franck-Condon factors, γ_{λ_2} was given a value of 0.12, whereas Z_{λ_2} and ϕ_{λ_2} were provided by the EMR company. Using the above values for the quantities γ, Y, Z, and ϕ results in a final calculated value of E_d of 1.7×10^{-5}. Finally, in assessing the value of V, a measured 0.10-cm^2 laser aperture was used which, on combining with an experimentally estimated value of l of 1.8 cm, resulted in a numerical value for V of 0.18 cm^3.

Taking the above values for E_{λ_1}, E_f, E_e, E_d, and V, the value of D_{λ_2} is calculated to be $D_{\lambda_2} = 2.6 \times 10^{-10}$ (NO), where (NO) is in units of molecules/cm^3. At an NO concentration of 1 ppbv this results in a calculated value of D_{λ_2} of ~7 photons/laser shot/PMT. The above theoretical estimate can be compared with the experimentally measured value of D_{λ_2} taken from Fig. 5 for 1-ppbv NO, which is also ~7 photons/laser shot/PMT. This surprisingly good agreement may, in fact, be somewhat fortuitous considering the combined uncertainty in our evaluation of Y_{λ_1} and V, and also in estimating the effective NO absorption cross section for our given laser conditions. This combined uncertainty could possibly range as high as ±2.0. Further refinement in some of our measuring techniques should hopefully reduce the uncertainty in the theoretical estimates to more like a factor of ±1.5 in the near future.

In future airborne field experiments involving the LIF NO detection system, the same collection optics package will be employed as used in the laboratory tests; thus all efficiency term values given above should have the same values in the field system. The one major change to be made in the field system will be the addition of five PMTs to the sampling chamber. Since the SP-LIF NO system is a signal-to-noise limited technique, this increase in PMTs can be expected to result in a further enhancement in the sensitivity for detecting NO of a factor of ~2.5. For this configuration the limit of detection for the field-sampling NO system is estimated at 8 pptv for an integration time of 20 min. (Still further improvements in the collection optics of the SP-LIF NO system and a further increase in the laser rep-rate could lead to yet another factor of 2 improvement in detection sensitivity.) A summary of the expected signal-to-noise ratios over a range of NO concentrations and for two different altitudes has been provided in Table I. From this it can be seen that a factor of 2 enhancement occurs in the NO detection sensitivity at high altitudes (e.g., 6 km), this being due to the reduction in the quenching of NO by O_2. Although well-established concentration values for natural tropospheric NO levels continue to elude the scientific community, it now appears that concentrations in the range of 3–300 pptv are the most probable (McFarland

Table I. SP-LIF NO Detection Sensitivity [a]—Based on Laboratory Calibration Curve but with Six PMTs Rather than One

Elevation: ground level			Elevation: free troposphere, 6 km (est)		
(NO) pptv	SNR 20 min	SNR 1 min	(NO) pptv	SNR 16 min	SNR 1 min
1200	360/1	80/1	1200	700/1	160/1
420	120/1	27/1	420	240/1	53/1
140	40/1	9/1	140	80/1	18/1
28	7/1	1.8/1	28	16/1	3.5/1
8	2/1 [b]		7	4/1 [b]	
			3.5	2/1 [b]	

[a] 226-nm laser energy, 1 mJ/pulse; rep-rate 10 psec.
[b] Extrapolated sensitivity.

et al.,[5] Kley *et al.*,[16] Kelly *et al.*,[17] Helas and Warneck,[18] and Schiff *et al.*[4]). If true, the SP-LIF methodology would seem to be well-suited to making significant contributions to the global data base.

Concerning the potential problem of chemical interferences, in field sampling conditions the two most likely interference candidates would now appear to be NO_2 and HNO_3; however, some consideration also needs to be given to HONO and PAN (peroxy-acetyl-nitrate). Both NO_2 and HNO_3 are known to be present in the daytime atmosphere at concentration levels well in excess of that for NO [i.e., $NO_2 \simeq 2(NO)$ and $HNO_3 \simeq 50(NO)$]. In each case, however, a two-photon absorption process is required for the interference to be detected:

$$\text{(a) } NO_2 + h\nu_1 \xrightarrow{(\lambda_1 = 226\text{ nm})} NO(v'' = 0) + O,$$

$$\text{(b) } HNO_3 + h\nu_1 \xrightarrow{(\lambda_1 = 226\text{ nm})} NO(v'' = 0) + HO_2,$$

$$\text{(c) } NO\ (v'' = 0) + h\nu_1 \xrightarrow{(\lambda_1 = 226\text{ nm})} NO^*,$$

$$\text{(d) } NO^* \rightarrow NO + h\nu_2 (\lambda_2 = 259\text{ nm}).$$

Thus far only NO_2 has been tested to determine the efficiency of the above two-photon process. The results from these experiments have shown that the NO fluorescence signal from NO_2 is ~100 times weaker than that from NO for the same concentration. This strongly suggests that in tropospheric conditions, the interference from NO_2 should be of negligible importance. Further experiments on the HNO_3 system as well as HONO and PAN are now being planned to establish an accurate upper interference limit for these species.

A second type of interference in the NO system could be that resulting from fluorescences from other atmospheric trace gases that might absorb significantly at 226 nm. This problem is actually not much different from that discussed earlier under the heading of white-fluorescence noise. Based on our current understanding of the chemical composition of the atmosphere, the most likely direct fluorescing species is expected to be SO_2. Thus tests designed to measure the level of SO_2 flourescence when excited at 226 nm, using NO collection optics, have been carried out. These tests have shown that for the same concentration levels the signal from SO_2 is ~20 times lower than that from NO. Hence, if all other factors were equal, one could operate the NO system in conditions where the atmospheric SO_2 level was 20 times larger than NO, with the final effect being that the experimentally measured NO signal would be a factor of 2 too high. This estimated interference level, however, does not take into consideration the fact that the NO excitaiton laser is tuned on and off the P_{11} NO bandhead, where a spectral change of 0.015 nm results in a decrease in the NO fluorescence signal of ≥8. This same laser tuning results in a decrease in the SO_2 fluorescence signal of only a factor of 1.12, the signal from SO_2 being higher when the laser is tuned off the P_{11} NO bandhead than on. Thus it now appears that NO/SO_2 concentration differences of a factor of ~50 could be tolerated without SO_2 presenting itself as a significant interference in the LIF measurement of NO. In the latter context, later in the text the authors discuss an LIF method of detecting SO_2 independent of any influence from NO. Also we note that Bradshaw and Davis[19] have reported a two-photon LIF NO system which results in blue-shifted NO fluorescence at 187 nm. The latter system completely avoids the SO_2 interference question and, in addition, appears to promise an increase in sensitivity over the SP-LIF NO system by a factor of ~14.

IV. Analysis of the SP-LIF SO_2 System

As noted earlier the laser hardware employed in the SP-LIF detection of SO_2 system was basically the same as that shown in Fig. 3. The only significant changes made in this system involved the type of dye used in the Quanta-Ray PDL, the removal of the 4-nm bandpass

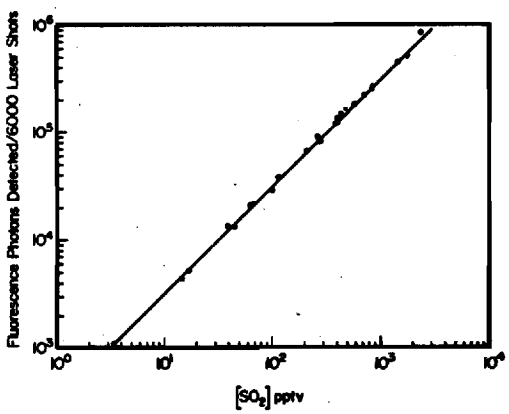

Fig. 6. Calibration curve for the detection of SO_2 via LIF, signal (photons/10 min integration time/PMT) vs SO_2 concentration (pptv). Asterisk data point corresponds to a sample in which air plus 13 Torr of water vapor was added. All other data points have been recorded in one atmosphere of air only. Concentration range covered 15 pptv–2 ppbv: Energy, 1 mJ at 222 nm.

filter, and the use of a cooled KD^*P frequency-mixing crystal rather the one operated at ambient temperature. The overall sampling scheme for SO_2 can be summarized as

$$SO_2X(^1A_1) + h\nu_1 \xrightarrow{(\lambda_1 = 222\ nm)} SO_2\tilde{C}(^1B)[\alpha_1(0,2)\text{transition}],$$

$$SO_2\tilde{C}(^1B) \xrightarrow{(\lambda_2 = 230\text{–}320\ nm)} SO_2X(^1A_1) + h\nu_2.$$

In this system SO_2 is excited into the $\tilde{C}(^1B_2)$ state, rather than the first excited singlet manifold [i.e., $\tilde{B}(^1B_1)$], due to the much shorter lifetime of the $C(^1B_2)$ state, e.g., ~45 vs 50 μsec for the first excited state (Hui and Rice[20]). As a result the value of E_f for the 222-nm pumping scheme is several orders of magnitude greater than that for pumping into the lower singlet state.

In contrast to the NO system the fluorescence from SO_2 occurs over a very broad spectral region, covering nearly 100 nm. However, in maximizing the SNR in this system it was found that the sampling bandwidth needed to be held to ~15 nm, with the center of the bandpass being spectrally located at ~260 nm. A second difference in the SO_2 system involves the contrast observed in the fluorescence signal when tuning the pumping laser on and off the peak absorption corresponding to the $\alpha_2(0,2)$ transition. In the SO_2 system this contrast ratio was a factor of ~6. The magnitude of the contrast factor for SO_2, in fact, turns out to be actually higher than expected based on existing UV absorption spectra for SO_2—see, for example, Hui and Rice.[20] In our experiments rotational fine structure could be resolved within the $\alpha_2(0,2)$ band, permitting a much higher contrast ratio than predicted. This rotational fine structure has also resulted in a significant increase in the effective SO_2 absorption cross section for the $\alpha_2(0,2)$ band; however, still larger values in the cross section could perhaps be realized in the future if the $\alpha_2(0,3)$ SO_2 band were pumped. This band has not been used in the present study since it is spectrally located at ~220.7 nm, and this wavelength can only be achieved with high efficiency using a frequency-mixing crystal operated at greatly reduced temperatures.

The calibration of the LIF SO_2 system was performed in the same fashion as discussed earlier for NO. Once again the dual-dilution dynamic-flow calibration system shown in Fig. 4 was employed in covering an SO_2 concentration range of 15 pptv–2 ppbv. However, to make possible an SO_2 calibration curve covering levels as low as 15 pptv, the diluent gas (i.e., either Scott or Linde air) had to be scrubbed in advance to mixing with the SO_2 standard. In the latter operation a dry ice/methanol slush bath was used in conjunction with a glass bead-filled U trap to remove residual SO_2.

The SO_2 calibration curve shown here in Fig. 6 was found to be linear over the entire concentration range of 15 pptv–2 ppmv. Once again there appears to be no fundamental limitations to the range of linearity over which this calibration curve could be taken provided appropriate optical-signal attenuators were to be systematically used at high concentrations. At one specific SO_2 concentration, namely, 450 ppbv, the quenching effect of H_2O was tested, with the results indicating, that at a concentration level of 13 Torr, the electronic quenching of SO_2 in the $C(^1B)$ state is primarily controlled by O_2 and N_2.

As in the case of NO, a semiquantitative evaluation of the signal strength can be made of the LIF SO_2 system by evaluating the various efficiency terms in Eq. (9). For the latter system we have calculated the values of E_{λ_1}, E_f, and E_e as follows:

$$E_{\lambda_1} = (\text{optical pumping efficiency at } 222\ nm) = 2.1 \times 10^{-2},$$

$$E_f = (\text{fluorescence efficiency}) = 1.4 \times 10^{-2},$$

$$E_e = 1.0.$$

The value of E_{λ_1} was here based on a laser energy of 1.0 mJ and an experimentally measured effective-absorption cross section for SO_2 at 222 nm (using the previously described laser system) of 1.7×10^{-18} cm^2, where this value is being defined as the product of $\sigma_{\lambda_1} \times f_i$. Based on a laser-energy dependence study we also were able to assign a value of unity to the quantity S_{λ_1}. The magnitude of the efficiency term E_f was calculated using available literature values for k_f, k_d, and $k_{q(\text{air})}$ as follows: $k_f = 1.8 \times 10^7$ sec^{-1} (Hui and Rice[20]); $k_d = 6.2 \times 10^6$ sec^{-1} (Hui and Rice[20]); and $k_{q(\text{air})} = 1.3 \times 10^9$ sec^{-1} (Okabe[21]). In evaluating the remaining two terms in Eq. (9), E_d and V, some of the same basic input was used as for the case of NO. For example, Y_{λ_2} was again taken to be 0.008, and a_{λ_2} and l were given the values 0.1 cm^2 and 1.8 cm, respectively; γ_{λ_2}, Z_{λ_2}, and ϕ_{λ_2}, on the other hand, were uniquely different for the SO_2 system having the values of 0.16, 0.33, and 0.12, respectively. The value of γ_{λ_2} was calculated based on a 15-nm passband centered at 260 nm; whereas the value of Z_{λ_2} was experimentally measured using the combined short- and long-wavelength cutoff solution filters. ϕ_{λ_2} was taken directly from the EMR calibration curve for our specific 541 Q PMT. Using the above values we calculated the final numerical value for E_d and V as

$$E_d = (\text{optical collection efficiency}) = 5.1 \times 10^{-5},$$

$$V = (\text{effective sampling volume}) = 0.18\ \text{cm}^3.$$

Thus based on the values of E_{λ_1}, E_f, E_e, E_d, and V, the magnitude of D_{λ_2} has been evaluated as $D_{\lambda_2} = 2.7 \times 10^{-9} \times (SO_2)$, where (SO_2) is in units of molecules/cm^3. At a given concentration of SO_2 of 1.0 ppbv the numerical value of D_{λ_2} is calculated to be $D_{\lambda_2} = 67$ photons/laser shot/PMT. This theoretically derived value of D_{λ_2} can be compared with the experimentally measured value taken from Fig. 6 for a concentration of 1.0 ppbv of fifty-five photons/laser shot/PMT. Thus we again find the agreement between our experimental and theoretical results quite good, but the authors again acknowledge that this might be fortuitous considering the still significant uncertainty in the evaluation of Eq. (9).

A comparison of the values of the efficiency terms in the SO_2 system with those calculated for the NO system shows that major differences exist between these two systems in three terms: E_{λ_1}, E_f, and E_d. E_{λ_1} is seen to be 1.4 times higher in the SO_2 system. E_f, on the other hand, is seen to be 2.3 times greater in the SO_2 system,

Table II. SO_2 Detection Sensitivity [a]—Based on Laboratory Calibration Curve

Elevation (ground level)			Elevation (free troposphere, 6 km)		
(SO_2) pptv	SNR 20 min	SNR 1 min	(SO_2) pptv	SNR 20 min	SNR 1 min
270	360/1	80/1	270	720/1	160/1
90	120/1	27/1	90	240/1	54/1
30	40/1	9/1	30	80/1	18/1
6	8/1[b]	1.8/1[b]	6	16/1[b]	3.6/1[b]
1.6	2/1[b]	—	1.6	4/1[b]	
			0.8	2/1[b]	

[a] Laser energy = 1.0 mJ (222.2 nm); rep-rate 10 pps, 6 PMTs; $\alpha_2(0,2)$ transition.
[b] Extrapolated sensitivity.

and E_d is 3 times larger in the case of SO_2. Thus it can be seen that with regard to signal strength alone the SO_2 SP-LIF system is ~9 times more sensitive than that for NO. On folding a somewhat higher noise level for the SO_2 system the limit of detection extrapolated from the SO_2 calibration curve is 4 pptv for an integration time of 20 min, using one PMT and a 222.9-nm laser energy of 1 mJ. Again this can be compared to a detection limit of 18 pptv for NO for the same energy of 1.0 mJ. Extrapolating the lab results shown in Fig. 6 to an airborne field sampling system, involving the same collection optics but 6 PMTs, results in a final limit-of-detection value of 1.6 pptv for a 20-min integration time. Given in Table II are the SNRs calculated for several different SO_2 concentrations at two different altitudes and for two different integration times. Comparing the SO_2 results summarized in Table II with several global SO_2 concentration values reported by Maroulis *et al.*[6] (e.g., typical boundary layer concentration values were 50 pptv, and typical free tropospheric SO_2 levels were 90 pptv for remote areas) one can conclude that the SP-LIF technique should have more than adequate sensitivity to detect SO_2 at virtually all geographical locations and at all tropospheric altitudes. Finally it should be noted that, at this time, the authors can identify no chemical interferences in the SP-LIF detection scheme for SO_2; however, a still more extensive examination is needed of perhaps certain sulfur-containing aromatic compounds. Okabe *et al.*[22] have examined the possibility of chemical interferences in an SO_2 fluorescence system, where the SO_2 excitation source used was either a cw-operated Zn or Cd atomic resonance lamp (213.8 and 228.8 nm, respectively). The sampling window (50 nm) in this system has centered at 350 nm. Compounds tested included CS_2, NO, NO_2, CO, CO_2, O_3, H_2S, C_2H_4, and CH_4. Of these, Okabe *et al.* found undetectable levels of interference for O_3, NO_2, CO_2, CO, CH_4, and H_2S for concentrations of these gases comparable with those found in a polluted atmosphere. In the case of NO, CS_2, and C_2H_4, the ratio of the SO_2 fluorescence signal to that from the above gases for equal concentrations was found to be 500/1, 500/1, and 4000/1, respectively. These data again suggest that it is unlikely that a serious chemical interference will be found in the SP-LIF detection scheme for SO_2.

The authors would like to acknowledge the support of this research by NSF grant ATM-7906556.

References

1. E. Barnett and Brodin, Tellus **7**, 251 (1955).
2. G. E. Likens, in Proceedings, Conference on Emerging Environmental Problems: Acid Precipitation; May, 1975, Rensselaerville, New York EPA Report 902/9-75-001.
3. B. A. Ridley and L. C. Howlett, Rev. Sci. Instrum. **45**, 742, (1974).
4. H. I. Schiff, D. Pepper, and B. D. Ridley, J. Geophys. Res. **84**, 7895 (1979).
5. M. D. McFarland, D. Kley, J. W. Drummond, A. L. Drummond, A. L. Schmeltekopf, and R. H. Winkler, Geophys. Res. Lett. **6**, 605 (1979).
6. P. J. Maroulis, A. L. Torres, A. B. Goldberg, and A. R. Bandy, J. Geophys. Res. **85**, 7345 (1980).
7. P. J. Maroulis, Ph.D. Thesis, Drexel U., Philadelphia, 1979.
8. H. Zacharias, A. Anders, J. P. Halpern, and K. H. Welge, Opt. Commun. **19**, 136 (1976).
9. A. C. Eckbreth, P. A. Bonczyk, and J. F. Verdicek, United Technologies Research Center Report R79-954403-13, Sept. (1978).
10. J. D. Bode, J. P. Carrico, and M. C. Johnson, Inst. Environ. Sci. Tech. Meet. Proc. **18**, 377 (1972).
11. D. D. Davis *et al.*, Rev. Sci. Instrum., 50, 1505 (1979).
12. I. S. McDermid and J. B. Laudenslager, "Radiative Lifetimes and Electronic Quenching Rate Constants for Single-Photon-Excited Rotational Levels of NO ($A^2\Sigma^+$, $v' = 0$)," J. Quant. Spectrosc. Radiat. Transfer (1982); in press.
13. L. A. Melton and W. Klemperer, Planet. Space. Sci. **20**, 157 (1972).
14. J. Brzozowski, P. Erman, and M. Lyyra, Phys. Scr. **14**, 290 (1976).
15. A. B. Callear and M. J. Pilling, Trans. Faraday Soc. **66**, 1618 (1970).
16. D. Kley, J. W. Drummond, M. McFarland, and S. Liu, J. Geophys. Res. **86**, 3513 (1981).
17. T. J. Kelly, D. H. Stedman, J. A. Ritter, and R. B. Harvey, J. Geophys. Res. **85**, 7417 (1980).
18. G. Helas and P. Warneck, J. Geophys. Res. **86**, 7283 (1981).
19. J. Bradshaw and D. D. Davis, Opt. Lett. **7**, 224 (1982).
20. Man-Him Hui and S. A. Rice, Chem. Phys. Lett. **17**, 474 (1972).
21. H. J. Okabe, J. Am. Chem. Soc. **93**, 7095 (1971).
22. J. H. Okabe, P. L. Splitstone, and J. J. Ball, J. Air Pollut. Control Assoc. **23**, 514 (1973).